X-ray diffraction evidence for epitaxial microcrystallinity in thermally oxidized SiO_2 thin films on the Si(001) surface

1993 J. Phys.: Condens. Matter 5 6525

(http://iopscience.iop.org/0953-8984/5/36/007)

J. Phys.: Condens. Matter 5 (1993) 6525–6536. Printed in the UK

X-ray diffraction evidence for epitaxial microcrystallinity in thermally oxidized SiO_2 thin films on the Si(001) surface

Isao Takahashi, Takayoshi Shimura and Jimpei Harada
Department of Applied Physics, Nagoya University, Chikusa-ku, Nagoya 464-01, Japan

Received 5 April 1993, in final form 15 June 1993

Abstract. In the x-ray diffraction pattern from a thermally oxidized thin film on an Si(001) surface, very weak Bragg peaks have been observed. The thermally oxidized thin film is, therefore, not purely amorphous but many small crystallites are dispersed within it, maintaining an epitaxial relation with the Si substrate. It is difficult to determine the structure of this crystalline phase because of the limited number of observable Bragg peaks. The pseudo-cristobalite structure proposed by Iida *et al* was selected as a possible model. The atomic arrangement is similar to that of the cristobalite structure, while the unit cell is tetragonal so as to match the lattice spacing to that of the Si substrate. A least-squares fitting analysis of the profile of the newly observed Bragg peak reveals that the crystallites are located not only at the interface between the Si substrate and the amorphous layer, but also widely distributed in the amorphous layer, preserving an epitaxial relation among the crystallites. The proportion of such crystallites is estimated to be a few percent of the whole volume of the amorphous layer.

1. Introduction

The structure of an amorphous silicon dioxide (abbreviated as a-SiO_2 hereafter) thin film on an Si wafer has been a subject of absorbing interest because of its unique role in semiconductor technology.

Several experimental studies aimed at understanding the nature of the a-SiO_2/Si interface have been performed using electron microscopy [1], x-ray diffraction [2, 3], and x-ray photospectroscopy [4]. The stable atomic configuration of a-SiO_2 on an Si(001) surface has also been a subject of theoretical study [5, 6]. However, the various experimental results mentioned above were not consistent with one another and also differed from the theoretical predictions. Such chaotic results are considered to arise partly due to sample-dependent phenomena. In order to study this problem, it would be necessary to systematically prepare a series of samples.

Recently, Iida *et al* [7, 8] reported that unknown x-ray diffraction peaks are observed in the crystal truncation rod (CTR) scattering from samples in which the surface is thermally oxidized, but not from samples in which the surface is chemically etched. They claimed that these peaks originated from crystalline scatterers which coexist in a-SiO_2, having some epitaxial relationship with the Si substrate, because of the variation of their intensity with thickness. We have extended this study in order to obtain more definite information about the structure of the crystalline phase, such as its crystallographic symmetry and its distribution in the a-SiO_2 film. In this paper, a more detailed description of these studies is reported on the basis of some additional experimental results.

0953-8984/93/366525+12$07.50

2. Experimental details

The present samples were prepared by heating Si(001) wafers by about 900 K in a dry oxygen atmosphere using a conventional oxidization facility as used in industry (Toshiba Co. Ltd). Several oxidized films with different thicknesses were prepared on the Si wafers by adjusting the oxidization time. The thickness of the film was estimated by measurement with an optical interferometer and from the x-ray reflectivity. The thermally oxidized layer on a wafer can easily be removed by etching the surface with an aqueous HF solution. These etched samples were also examined in order to compare the results with those of the thermally oxidized ones.

For the measurement of the x-ray scattering, a four-circle diffractometer (laboratory made) installed on a rotating-anode x-ray generator (Rigaku RU-200) was used in which Cu Kα radiation was monochromated by pyrolitic graphite. For high-resolution measurement the Huber four-circle diffractometer with an Si crystal analyser installed on BL-4C at the Photon Factory, KEK, Tsukuba was used. In addition, Sakabe's camera with an imaging plate detector installed on the BL-6A2 were also used for investigating the whole aspect of the x-ray diffraction pattern in reciprocal space. The wavelength was chosen to be 1.54 Å and the experiments were carried out at room temperature and atmospheric pressure.

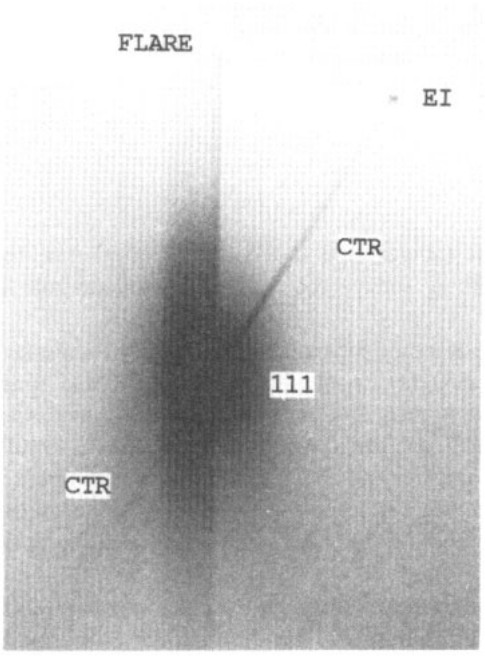

Figure 1. Oscillation photograph taken around the 111 Bragg point of the Si(001) wafer using an imaging plate detector mounted on Sakabe's Weissenberg camera at BL-6A2, Photon Factory, KEK. The large central spot is the 111 Bragg reflection of the Si substrate, and the sharp line extending from it is the CTR scattering. The enhancement of intensity is recognized near the point $(1, 1, 1-q)$ denoted as EI. As for the FLARE, we refer the reader to a detailed discussion of this phenomenon by Shimura *et al* [12].

3. Results

The characteristic features of the x-ray diffraction peaks found in the previous works [7, 8] are summarized as follows.

(1) There is an intensity enhancement at the point $(1, 1, 1-q)$ and at its equivalent points in reciprocal space, where q (about 0.54) is the distance in reciprocal space from the 111 Bragg point. The value of q depends slightly on the thickness and oxidation process. Such an intensity enhancement was not observed around the 202, 311, 331, and 000 Bragg points.

(2) The enhancement of intensity is exactly located on the line of the CTR scattering as demonstrated in the oscillation photograph shown in figure 1. We see clearly that it is not correlated with any other scattering, such as the halo pattern from a-SiO_2.

(3) The FWHM of the peak in the direction perpendicular to the CTR is of the same order of magnitude as those of the Bragg reflection and the CTR scattering observed from the Si substrate. The geometric relation among the Si(111) Bragg reflections, CTR scattering, and the newly observed peaks is schematically represented in figure 2.

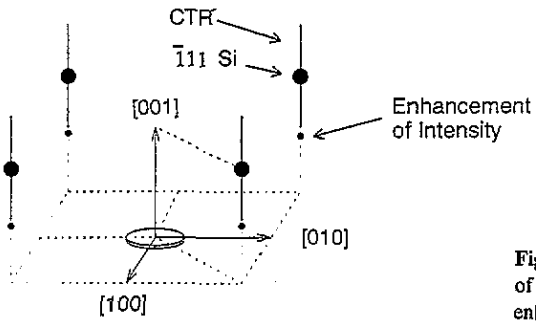

Figure 2. Schematic representation in reciprocal space of the 111 Bragg reflection, the CTR scattering, and the enhancement of the intensity from the oxidized layer.

(4) The peak intensity depends on the thickness of the a-SiO_2 layer and is not observed in the etched samples.

(5) The high-resolution measurement shows that the profile of the peak intensity along the CTR scattering has fine structure. In figure 3 the results obtained from two samples with different thicknesses of the oxidized layer are shown. The profiles show Laue-function-like fringe patterns, although their intensities are very weak and asymmetric with respect to the peak position. The distance between the adjacent interference fringes approximately corresponds to the inverse of the film thickness.

From these results it is understood that the enhancement of the intensity at the point $111-q$ is a kind of Bragg scattering from a crystalline phase which exists in the a-SiO_2 layer. Moreover, from the value of the FWHM and from the period of the interference fringes, it is deduced that the size of the crystalline phase would be almost the same as that of the amorphous layer. However, if such a large volume is completely occupied by the crystalline phase, the peak intensity should be much stronger than the observed one. Consequently, the crystalline scatterers are considered to be distributed all over the thin oxide film, having an epitaxial relation with the Si(001) substrate and also with one another.

If the above interpretation is acceptable, the lateral lattice spacing of the crystalline scatterers is to be matched to that of the Si substrate and the spacing along the direction normal to the surface must be elongated and is estimated to be about $[1/(1-q)]a_{Si}$, where a_{Si} is the lattice constant of the Si crystal.

4. Structure of crystalline scatterers in a-SiO_2

In general the average structure of a crystal can be determined from the analysis of the

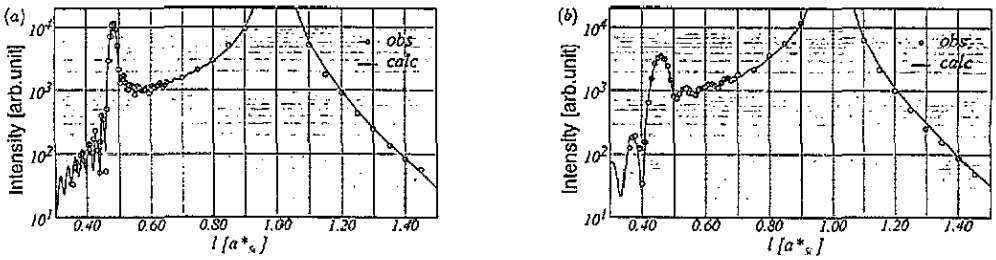

Figure 3. Intensity profiles plotted along the $11l$ line on the CTR scattering, measured by high-resolution diffractometer at BL-4C, Photon Factory, KEK: (*a*) for sample A, and (*b*) for sample B. The thicknesses of the a-SiO_2 layers are 250 Å and 112 Å, respectively, for samples A and B.

intensity distribution of the Bragg reflections in reciprocal space. The reliability of the structure determined depends on the number and accuracy of the Bragg reflection intensities used in the analysis. In the present case the number of non-equivalent Bragg reflections observed is only one, so it is apparently not sufficient to perform ordinary structure analysis.

An attempt has been made by Iida *et al* [7] to differentiate among the structural models so far proposed for the interface structure between the a-SiO_2 and Si(001) surface [1, 2, 4–6] in the light of their observations. Figure 4 shows the unit of the structure selected by them as one of the most probable interface structures. The atomic arrangement is essentially the same as that of the β-cristobalite structure of the cubic system, except that it is tetragonally deformed: the lattice is elongated along the c axis so as to fit the lateral lattice spacing to that of the Si substrate [7] and to keep the bond distance between the Si and O at about 1.6 Å. This structure is represented by space group $I4_1/amd$ of the tetragonal system of the unit cell with $\sqrt{2}a_{PC} = a_{Si}$ and $c_{PC} = a_{Si}/(1-q) \equiv sa_{Si}$. The intensity enhancement at the observed point $111-q$ is well reproduced by this model. As pointed out by Iida *et al* [7], however, this model also enhances the intensity near the 004 and 202 Bragg points, contrary to observations. Thus, some modification should be made before accepting this model. It is not difficult to see that the above additional extinction rule for the 004 and 202 reflections is satisfied even for this model, if half the number of scatterers are situated in anti-phase relation with the other. Such anti-phase scatterers are in fact expected to exist on the (001) interface, because there are several different step levels on the (001) interface of the Si substrate. The existence of the anti-phase steps is verified by comparing the CTR intensity emanating from the 111 Bragg point with that from the $1\bar{1}1$ Bragg point, because they should be different if the surface is ideally flat, as pointed out by Kashihara *et al* [9]. A good agreement between those two CTR scattering intensities was experimentally confirmed for the Si(001) wafers [9].

Once we have the model, it is possible to estimate the intensities of other reflections on the basis of the model including the anti-phase scatterers. The calculated intensities are listed in table 1. From this table we notice that the intensity of the $111-q$ reflection is prominent. Thus, we can see the reason why it is not easy to observe other reflections. Moreover, it is conceivable that the epitaxial crystalline scatterers are not properly aligned but randomly distributed even in the a-SiO_2 layer by maintaining an epitaxial relation with one another as will be described in the next section. Thus the static Debye–Waller factor for such a misaligned structure may be considerable and may reduce the intensity of higher-order reflections below the calculated values listed in table 1. It would also be one of the

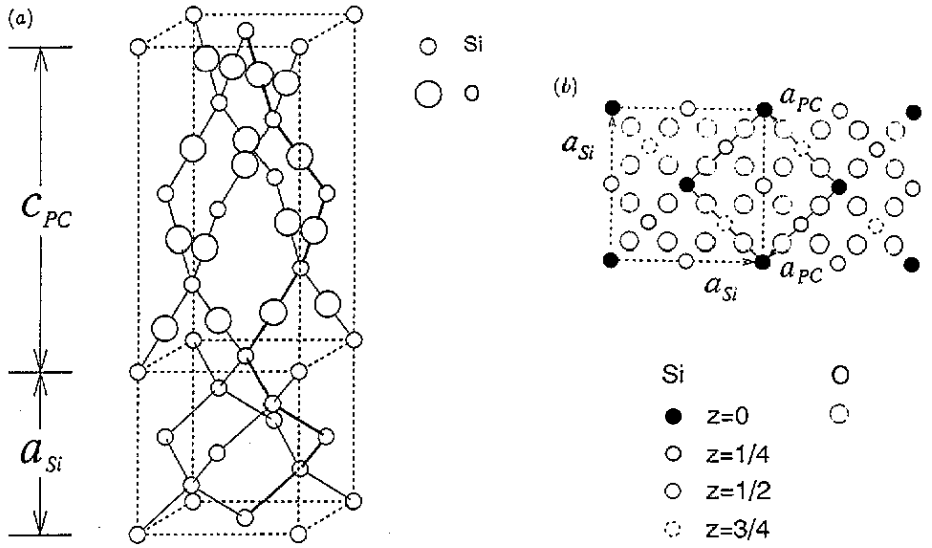

Figure 4. Epitaxial relationship between the pseudo-cristobalite and the Si(001) substrate (*a*) and its projection along the *c* axis (*b*). a_{Si}, a_{PC}, and c_{PC} represent the unit cell parameters of Si and the tetragonal pseudo-cristobalite crystal, respectively. The space group is $I4_1/amd$ (No 141). Si atoms are located on the 4*a* position and O atoms are on the 8*c* position in Wyckoff's notation.

Table 1. Intensities calculated on the basis of the epitaxial pseudo-cristobalite structure for SiO_2 and the Si substrate by using the refined parameters in model III of table 2. $I_{PC}/I_{TOTAL} > 0.1$ are indicated, where $I_{PC} = |\langle\Phi_{PC}\rangle|^2$, $I_{TOTAL} = |\langle\Phi_{Si}\rangle + \langle\Phi_{PC}\rangle|^2$, and $I_{CTR} = |\langle\Phi_{Si}\rangle|^2$.

h	k	l	I_{TOTAL}	I_{PC}	I_{CTR}
0	0	$8-8q$	1863	825	225
1	1	$1-q$	4280	3608	119
1	1	$7-7q$	73	591	311
1	1	$9-9q$	11	6	1
2	0	$2-2q$	33	24	1
2	0	$10-10q$	6	5	1
2	2	$2-2q$	18	20	1
2	2	$4-4q$	21	17	1
2	2	$6-6q$	7	2	2
2	2	$8-8q$	648	166	167
2	2	$10-10q$	25	3	11
3	1	$1-q$	196	49	64
3	1	$3-3q$	436	161	144
3	1	$5-5q$	30	67	8
3	1	$7-7q$	105	30	230

reasons why other higher-order reflections have not been observed.

5. Distribution of crystalline scatterers

The distribution of scatterers in some limited space is reflected in the profile of the peaks scattered from it. Thus the analysis of the profile makes it possible for us to deduce the

Table 2. The parameters used and refined in model (III). Refined parameters are given, together with the estimated standard deviations in parentheses. The isotropic thermal parameters B_{Si} and B_O were kept at 0.45 and 0.60 Å^2, respectively.

	Sample A	Sample B
R factor	0.040	0.062
Weighted R factor	0.065	0.079
Number of intensities	74	47
k	1.23(1)	1.37(2)
$\langle \delta p^2 \rangle$	0.074(7)	0.10(1)
ρ_0	0.060(4)	0.067(9)
ρ_1	0.062(1)	0.067(4)
ξ	21(1)	14(4)
P_{max}	21	7
Δc	0	0
$s(= 1/(1-q))$	2.077(1)	2.226(5)
u_0	0	0

distribution of the scatterers. As the extra peak observed is reproduced by introducing crystallite scatterers with the pseudo-cristobalite structure, we assume that such scatterers are dispersed randomly in the a-SiO_2 film, although they maintain an epitaxial relationship with the Si substrate.

5.1. Intensity expression

The intensity distribution of CTR scattering is proportional to the square of the average column scattering factor $\langle \Phi(\boldsymbol{K}) \rangle$ [10]:

$$I(\boldsymbol{K}) = [\mathrm{Lp}][\mathrm{Re}][\mathrm{A}]|\langle \Phi(\boldsymbol{K}) \rangle|^2 L(K_x) L(K_y) \tag{5.1}$$

where $\langle \ldots \rangle$ means to take the average of ... over the lateral x and y directions, $L(K_x)$ and $L(K_y)$ are the Laue functions for the x and y directions of the scattering vector $\boldsymbol{K} = (K_x, K_y, K_z)$ ($K = 4\pi \sin\theta/\lambda$), respectively, and [Lp], [Re] and [A] are the Lorentz polarization factor, the resolution correction, and the correction for the effective area for scattering, respectively [11]. It is possible to select a spiral chain connected by the bold lines [9] shown in figure 4(a) as the column scatterer to the present case, where the z axis is taken to be normal to the interface and its origin at the interface. Thus, the region of negative z means that the inside of the Si substrate and the region of epitaxial crystallites on the substrate is in the region of positive z. The average column scattering factor $\langle \Phi(\boldsymbol{K}) \rangle$ is given as the sum of the column scattering factor from the Si substrate and that from the pseudo-cristobalite, by taking into account the phase relation between the two,

$$\langle \Phi(\boldsymbol{K}) \rangle = \langle \Phi_{Si}(\boldsymbol{K}) \rangle + \langle \Phi_{PC}(\boldsymbol{K}) \rangle \exp(\mathrm{i} K_z \Delta c) \tag{5.2}$$

where $\Phi_{Si}(\boldsymbol{K})$ and $\Phi_{PC}(\boldsymbol{K})$ are the column scattering factors for the Si substrate and pseudo-cristobalite, respectively, and Δc is the lattice mismatch between the two. $\Phi_{Si}(\boldsymbol{K})$ is given in terms of the structure factors $F_{Si}(\boldsymbol{K})$ of Si for the unit in a column as

$$\Phi_{Si}(\boldsymbol{K}) = k F_{Si}(\boldsymbol{K}) \sum_{p=0}^{-\infty} \exp[\mathrm{i} K_z p (a_{Si} + u_p)] \tag{5.3}$$

where k is a scale factor, p is the integer representing the Si lattice site pa_{Si} along the z direction and u_p is the lattice relaxation at the pth cell from the interface. If only the

uppermost cell at the interface has a lattice relaxation ($u_0 \neq 0$ and $u_p = 0$ for $p \neq 0$), the average column scattering factor is written as

$$\langle \Phi_{Si}(K) \rangle = F_{Si}(K)\{1/[1 - \exp(-iK_z a_{Si})] + iK_z u_0\}\Gamma(K_z). \tag{5.4}$$

This is the CTR scattering term from the Si substrate including the lattice relaxation u_0 at the top surface and $\Gamma(K_z)$ is the roughness damping factor (RDF) for the interface [10] which may be written in the form

$$\Gamma(K_z) = \sum_{p=-\infty}^{P_{max}} \gamma_p \exp(iK_z p a_{Si}) \tag{5.5}$$

where γ_p is the relative area of the pth level to the whole area of the interface. In the present analysis, this damping factor was approximated by introducing a roughness parameter $\langle \delta p^2 \rangle$ [10] near the 111 Bragg point,

$$\Gamma(K_z) = \exp[-\langle \delta p^2 \rangle (2\pi - a_{Si} K_z)^2/2]. \tag{5.6}$$

As for the epitaxial scatterers, $\Phi_{PC}(K)$ is written by

$$\Phi_{PC}(K) = F_{PC}(K) \sum_{p=1}^{P_{max}} \rho(p) \exp\{iK_z p[c_{PC} + \delta c_{PC}(p)]\} \tag{5.7}$$

where $\rho(p)$ is the probability of finding crystallite on the pth level from the interface in the pseudo-cristobalite with cell parameter c_{PC}. $\delta c_{PC}(p)$ is the displacement of the scatterer at the pth level along the direction normal to the interface, but it is considered that δc_{PC} does not change systematically with the level p nor with the x, y coordinates.

In the present study the following three models were considered for the distribution of the crystalline scatterers $\rho(p)$. The distribution models are schematically shown in figure 5.

(I) Uniform distribution model: the scatterers are distributed uniformly from the interface up to the P_{max}th layer height.

$$\begin{aligned} &\rho(p) = \rho_1 \qquad \text{for } 1 \leqslant p \leqslant P_{max} \\ &\rho(p) = 0 \qquad \text{for } p > P_{max}. \end{aligned} \tag{5.8}$$

(II) Exponential distribution model: the density of the scatterers decreases with the distance from the interface in an exponential form,

$$\rho(p) = \rho_1 \exp(-p/\xi) \qquad \text{for } 1 \leqslant p \leqslant P_{max}. \tag{5.9}$$

(III) The combination of models (I) and (II): the scatterers are predominantly distributed at the interface and then their distribution changes with the distance from it in a similar way to the case of model (II).

$$\begin{aligned} &\rho(p) = \rho_1 + \rho_0 \qquad \text{for } p = 1 \\ &\rho(p) = \rho_1 \exp(-p/\xi) \qquad \text{for } 1 < p \leqslant P_{max}. \end{aligned} \tag{5.10}$$

For these three cases the average column scattering factor is written as

$$\begin{aligned} \langle \Phi_{PC}(K) \rangle = F_{PC}(K)\{&\rho_0 + \rho_1\{1 - \exp[P_{max}(iK_z c_{PC} - 1/\xi)]\} \\ &\times [1 - \exp(iK_z c_{PC} - 1/\xi)]^{-1}\}\Gamma_{PC}(K) \end{aligned} \tag{5.11}$$

where $\Gamma_{PC}(K)$ is the static Debye–Waller factor due to $\delta c_{PC}(p)$ in a form of Gaussian function. $\rho_0 = 0$ and $\xi = \infty$ for model (I), and $\rho_0 = 0$ for model (II).

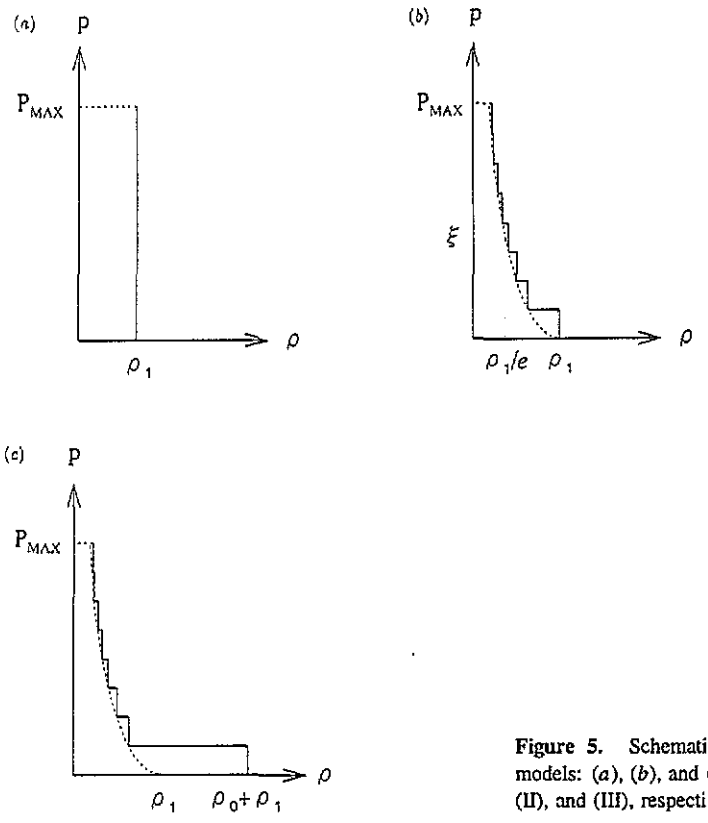

Figure 5. Schematic representation of distribution models: (*a*), (*b*), and (*c*) correspond to the models (I), (II), and (III), respectively.

5.2. *Least-squares refinement*

In the refinement we took into account the coherent contributions from the anti-phase epitaxial regions to the intensity I_j following Kashihara *et al* [9], and a function $\Sigma w_j[I_j(\text{calc}) - I_j(\text{obs})]$ was minimized, where w_j is the weighting factor $1/I_j$. In the refinement, we ignored the contribution of the static Debye–Waller factor $\Gamma_{PC}(\boldsymbol{K})$, regarding it as a constant term, because the analysis was made for one Bragg reflection. There are many combinations of different choices of parameters, but some common features were recognized after some refinement: the refinement of the roughness parameter $\langle\delta p^2\rangle$ always converged to a small value, suggesting that the interface between the Si substrate and the epitaxial crystallites is sufficiently flat except for the existence of the anti-phase steps. This result is in accordance with the observation by transmission electron microscopy (TEM), as mentioned later. Although the mismatch parameter Δc was introduced, no improvement was obtained in the refinement, indicating the refinement to be insensitive to this parameter.

The best-fit results obtained for the three models are shown in figure 6. We see that even though model (I) is the simplest one of the three, the qualitative aspects of the observed profile are well predicted: each fringe position is in agreement with the observation and the intensity asymmetry around the main peak is also in the right sense. In the case of model (II), the intensity modulation seen at the higher-angle side from the main peak is very much improved by introducing the exponential-type decay function for the distribution. However, the intensity asymmetry is so much exaggerated in this model that the agreement becomes rather poor in the weak-intensity region at the low-scattering-angle side. In model (III),

such a disagreement is well overcome as shown in figure 6(*c*), suggesting that the epitaxial crystalline scatterers exist with high density especially on the interface.

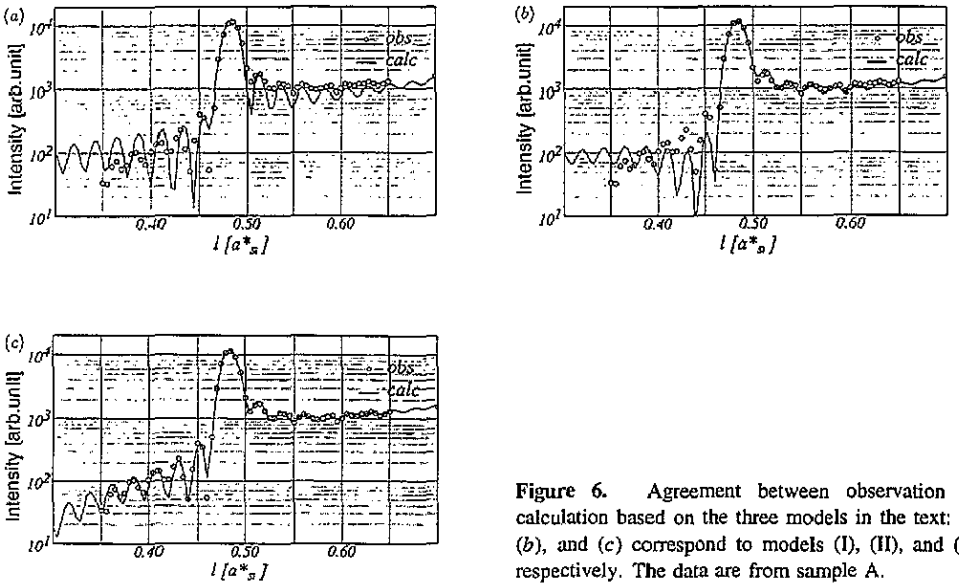

Figure 6. Agreement between observation and calculation based on the three models in the text: (*a*), (*b*), and (*c*) correspond to models (I), (II), and (III), respectively. The data are from sample A.

Since the refinement on the basis of model (III) went successfully for sample A, a similar refinement was examined for sample B. The difference between the two samples is in the thickness of the a-SiO_2 layer on the substrate. A satisfactory refinement was also achieved for this sample. The agreements with the whole observed profiles including the CTR scattering for samples A and B are shown by full curves in figure 3(*a*) and (*b*), respectively, and the parameters obtained in the refinement are listed in table 2. We may imagine from this refinement that the proper distribution of the crystalline scatterers in the oxide film is really of the form given by model (III).

Throughout the refinement, the thermal parameters of Si and O atoms were kept constant; their values were taken from their bulk values.

6. Crystalline state in a-SiO_2

From the parameters refined on the basis of model (III), it is possible to elucidate several important features of the crystalline state in the a-SiO_2 film. The probability of finding crystallites is predominantly high at the interface as the parameter $(\rho_0 + \rho_1)/k$ is 0.10 for model (III). At the second layer it becomes a few percent and then decreases further with the distance from the interface, suggesting that the epitaxial crystallites are only formed at the interface during the oxidization process and that a portion of them exist in the amorphous oxide film while maintaining an epitaxial relation with the substrate. Such an oxidization process is illustrated schematically in figure 7. The concentration of the epitaxial crystallites is very low compared with the whole volume of the a-SiO_2 phase as expected from section 3.

If we look more closely at the structure of pseudo-cristobalite in the a-SiO_2 film, it is recognized that the structure consists of unusually small and large bond angles of O–Si–O

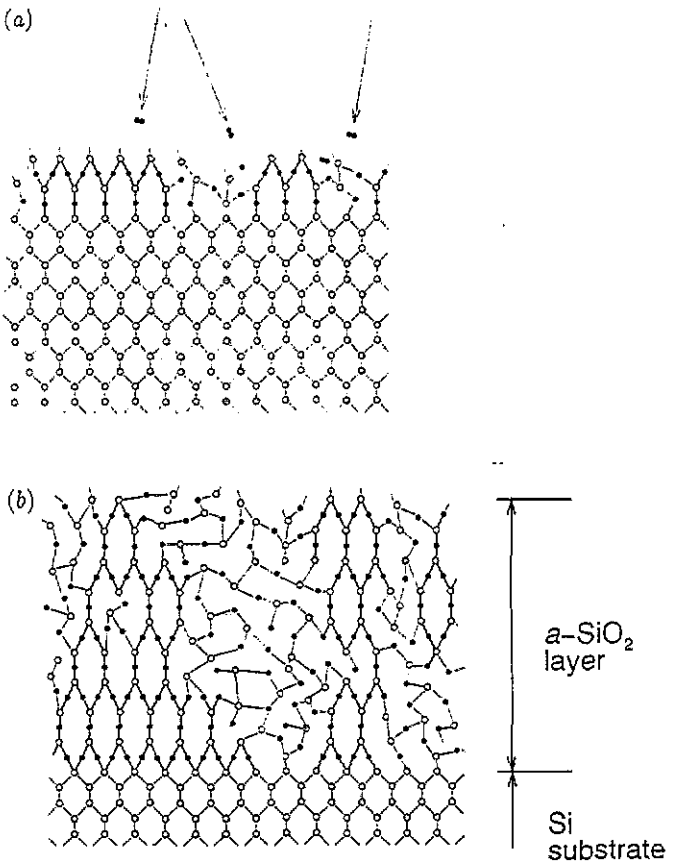

Figure 7. Schematic representation of the oxidization process of an Si(001) wafer. (*a*) After oxygen molecules arrive on the Si(001) surface, epitaxial crystallites of the pseudo-cristobalite structure are partially formed at the interface. (*b*) By further oxidization, the interface itself will move into the interior of the substrate. Some of the crystallites may transform into the amorphous structure; meanwhile, new epitaxial crystallites are formed at the new interface. Thus at the final stage of oxidization, the epitaxial crystallites of pseudo-cristobalite structure are predominantly distributed at the interface but some are in the amorphous oxide film, maintaining an epitaxial relation. In this figure, the amount of crystallites is exaggerated.

such as about 65° and 135°, respectively. It is suspected from this unfamiliar structure that the crystallites are probably unstable. Thus, this leads us to imagine that the formation of the crystalline SiO_2 phase would only be stabilized as the result of highly stressed circumstances near the SiO_2/Si interface. The formation of such an epitaxial layer is supposed to depend on the process of oxidization of Si wafers. Under such a circumstance, even the unit-cell size along the *c* axis of each crystallite may not be well defined, although the average unit-cell size of the *a* and *b* axes should be matched to the period of the substrate. Therefore the unit-cell size along the *c* axis varies around the average value in the amorphous layer. Actually, as indicated in table 2, the *s* value is different for samples A and B. We have recently examined how the distribution of the epitaxial crystallites in the oxide film differs depending on the oxidization condition. An interesting result with respect to the oxidization process has been obtained by this experiment, which will be reported in a separate paper.

7. Concluding remarks

In order to confirm the evidence obtained by x-ray diffraction, the crystallites were examined using a transmission electron microscope (TEM). The sample was prepared using the well known technique for cross-sectional observation. However, no confirmation of crystallite existence was observed, although good quality lattice images were recorded, even though the area of observation was selected so as to include the interface boundary.

One possible reason why the crystallites could not be seen by the TEM is that the mean size of the crystallites may be of the order of the unit-cell size or less as suggested before, although crystallites have epitaxial relationships one with another and also with the Si substrate. Another explanation would be possible: the crystallites are considered to be very unstable so that the sample preparation for the TEM observation was too harsh to keep the crystallites stable. Thus, almost all the crystallites might be transformed into the amorphous state during the process of sample preparation. This hypothesis would be in keeping with the above discussion that the formation of unstable pseudo-cristobalite would be favoured under stress existing at the strained interface.

The mechanism of electronic breakdown of the oxide film on Si wafers is a very interesting subject, but the relationship between the crystallites which are proposed to exist from the present x-ray study and the mechanism for the electric breakdown of the oxidized film is not yet clear, although the present work indicates that the structure of the a-SiO_2 film grown on Si wafers appears not to be uniform and also not to be ideally simple on an atomic scale.

Acknowledgments

The authors wish to express their thanks to Mr Y Iida of Toyota Automobile Co. Ltd and Mr S Samata and Mr Y Matsushita of Toshiba Co. Ltd for their collaborations at an early stage of the present study, and also to K Nakano and M Takata of the authors' group, and to Professor N Tanaka of Nagoya University, for their assistance in calculations and in performing the TEM experiment, respectively. The high-resolution x-ray measurements were performed at the Photon Factory, KEK under the proposal No 90-086; we also thank Professor T Sakabe, Dr A Nakagawa and Dr S Kishimoto of KEK for their assistance. Part of the computer calculation was performed at Nagoya University Computing Centre. This study was supported by Grants-in-Aid for scientific research on priority areas Nos 03243105 and 04227105 from the Ministry of Education and Culture, Japan.

References

[1] Ourmazd A, Taylor D W and Rentschler J A 1987 *Phys. Rev. Lett.* **59** 213
[2] Fuoss P H, Norton L J, Brennan S and Fischer-Colbrie A 1988 *Phys. Rev. Lett.* **60** 600
[3] The present authors think that the broad peak reported in [2] is more likely to be characteristic thermal diffuse scattering of the Si single crystal due to transverse phonons of relatively low frequency at the Brillouin zone boundary.
[4] Hattori T, Igarashi T, Ohi M and Yamagishi H 1989 *Japan. J. Appl. Phys.* **28** 1436
[5] Tiller W A 1981 *J. Electrochem. Soc.* **128** 689
[6] Hane M, Miyamoto Y and Oshiyama A 1990 *Phys. Rev.* B **41** 12 637
[7] Iida Y, Shimura T, Harada J, Samata S and Matsushita Y 1991 *Surf. Sci.* **258** 235
[8] Harada J, Iida Y, Shimura T, Samata S and Matsushita Y 1991 *Proc. Symp. on Advanced Science and Technology of Silicon Materials (145th Committee Japan. Soc. Promotion Sci.)* (Tokyo: Japan. Soc. Promotion Sci.) p 309

[9] Kashihara Y, Kawamura K and Harada J 1991 *Surf. Sci.* **257** 210
[10] Harada J 1992 *Acta Crystallogr.* A **48** 764
[11] Robinson I K 1988 *Aust. J. Phys.* **41** 359
[12] Shimura T and Harada J 1993 *J. Appl. Crystallogr.* at press